ELECTROLUMINESCENCE AND THERMAL IMAGING OF DEFECTS IN THIN-FILM CHALCOPYRITE SOLAR CELLS

Ľubomír Škvarenina
Doctoral Degree Programme (3), FEEC BUT
E-mail: skvarenina@phd.feec.vutbr.cz

Supervised by: Robert Macků
E-mail: macku@feec.vutbr.cz

Abstract: Thin-film chalcopyrite based Cu(In, Ga)Se_2 solar cells with a metal wrap through interconnection were investigated by non-destructive methods in our research. The primary focus of this investigation was a detection and a localization of microstructural defects in this type of Cu(In, Ga)Se_2 solar cells. A combination of a visible and near infrared electroluminescence with a lock-in thermography was used for these purposes. Mainly the electroluminescence was a very sensitive tool for an indication of pre-breakdown sites influenced by a trap-assisted tunneling or stress-induced leakage currents. A strong correlation between electroluminescence maps and lock-in thermograms was obtained after a local breakdown accompanied by a creation of permanent defect.

Keywords: thin-film, CIGS, IR lock-in, electroluminescence, metal wrap through

1. INTRODUCTION

Chalcogenide solar cells became a most promising technology for a commercial production in the thin-film photovoltaics. Today the best laboratory efficiency of a Cu(In, Ga)Se_2 technology is 22.6 % and 22.1 % of CdTe thin-film devices. Despite the technological advancement of the chalcopyrite Cu(In, Ga)Se_2 solar cells structure, the wide range of physicochemical properties of particular defects still is not sufficiently explored and explained. The chalcopyrite Cu(In, Ga)Se_2 solar cells used in this investigation are formed on a substrate from an aluminum foil with metal wrap through (MWT) architecture [1]. This structure is based on grid contacts through the Al substrate with Mo/CIGS/CdS/-*i*-ZnO/ZnO:Al layers which are connected to the rear side formed by a second Al foil with a thin Al_2O_3 layer. An insulating carrier substrate layer between the Al foils is formed by a polyethylene terephthalate (PET). The principle of the Cu(In, Ga)Se_2 solar cell is equivalent to conventional c-Si solar cells. Radiation is absorbed near the *pn*-junction which generates electrons and holes. Then the electrons are collected by a transparent conductive layer of ZnO:Al/*i*-ZnO from an interface through an *n*-type buffer layer of CdS. Similarly, the holes are collected by a Mo electrode layer from an interface through a *p*-type absorber layer of Cu(In, Ga)Se_2 [2].

2. EXPERIMENTAL SYSTEMS

Measurements of dark current density-voltage (J–V) characteristics were performed by a source meter Keithley 2420 in a thermally insulated box. A stabilization of an ambient temperature (T_A) was ensured by a Keithley 2510 TEC. These basic measurements had to be done for an estimation of a suitable voltage bias which was essential to a performance of next presented methods. Experimental systems based on a CCD camera and a thermal imager were used for an investigation of radiation maps presented in section 3. A sensing of the CCD camera was ensured by a cooled 3.2 MPx Si-chip in a spectral range from 300 nm to 1100 nm. This visible and near-IR investigation was supplemented by a sensing of radiation in the far-IR spectral range from 7.5 µm to 13 µm by a lock-in technique.

Thermal imager used for this technique was equipped with an uncooled focal plane array with a resolution of 120 × 160 pixels. The method was realized like a periodically pulsed current-bias in a combination with a measurement of the surface temperature modulation as in [3]. Implementation of an air cooling of samples was highly necessary to ensure a better signal-to-noise ratio during iterations of measurements. A voltage bias was applied by a power supply Agilent E3631A. A scanning electron microscopy (SEM) was used for a detailed exploration of an MWT cross-section and a searching of microstructure defects on the surface. Epoxy resin mounting of samples in combination with a grinding/fine-polishing was used for a preparation of a high-quality cross-section of the MWT architecture. The multilayer structure was explored additionally by using a focused ion beam.

3. RESULTS AND DISCUSSION

The samples were prepared from a solar cell sheet by a mechanical segmentation. The non-uniformities were created along the segmented edges such as fractures through Mo/CIGS/CdS/*i*-ZnO/ZnO:Al layers and disruption at grain boundaries of the polycrystalline active layer $Cu(In,Ga)Se_2$. These non-uniformities provide the numerous parasitic current pathways which caused a leakage current between a back contact of Mo and a front transparent conductive oxide of ZnO:Al. The leakage current at the edges was very significant and have a strong influence on the *J–V* characteristics of the prepared samples. Therefore it was highly necessary to delete entire edges by a precision grinding and fine polishing. Forward and reverse dark *J–V* characteristics of three prepared samples are showed in Fig. 1. Presented characteristics were measured of course after the edge deletion. The measurements were performed several times for a stability verification and time independence of the obtained results. The following discussion will be focused on the sample marked as $^{NS}CIGS_3$ in Fig. 1.

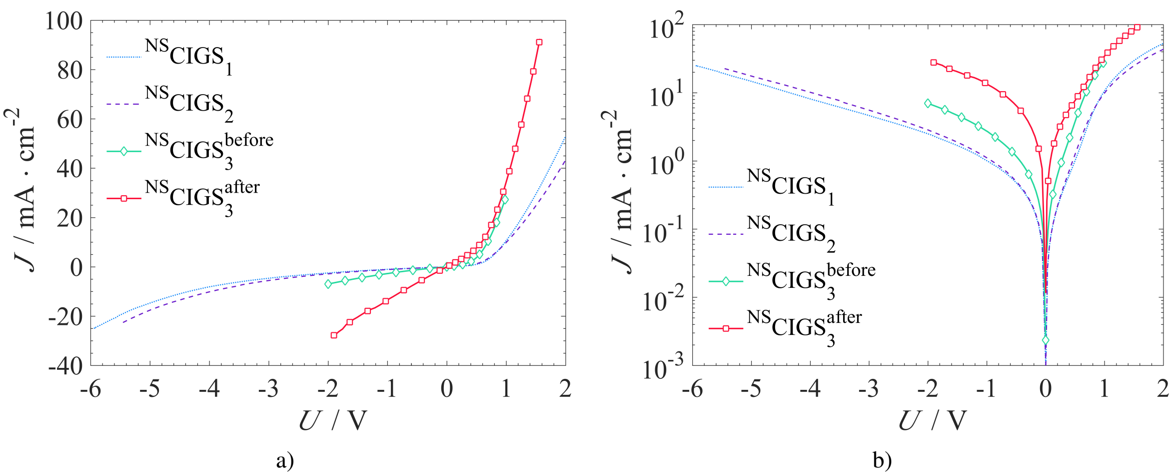

Figure 1: Dark *J–V* characteristics of thin-film $Cu(In,Ga)Se_2$ solar cell samples with an MWT architecture in a) linear and b) semilogarithmic scale, T_A = 301.15 K.

A sensitive method to detect and localize defects or impurities in semiconductors was based on the analysis by an electroluminescence intensity mapping under a dark condition [4]. The created fractures at the edges were often observed as a radiation along the edges before their deletion. Therefore the electroluminescence was used not only for a systematic investigation of defects in the bulk but also for quality evaluation of deleted edges. During the electroluminescence measurement was observed a local breakdown which created a permanent defect in the bulk. The electroluminescence map of the sample before the local breakdown is showed in Fig. 2a for applied forward bias and in Fig. 2b for a reverse bias. The visible dark spot at forward-bias marked as “A” was a type of defect also observed at samples $^{NS}CIGS_1$ and $^{NS}CIGS_2$. A radiation of this defect was visible only in

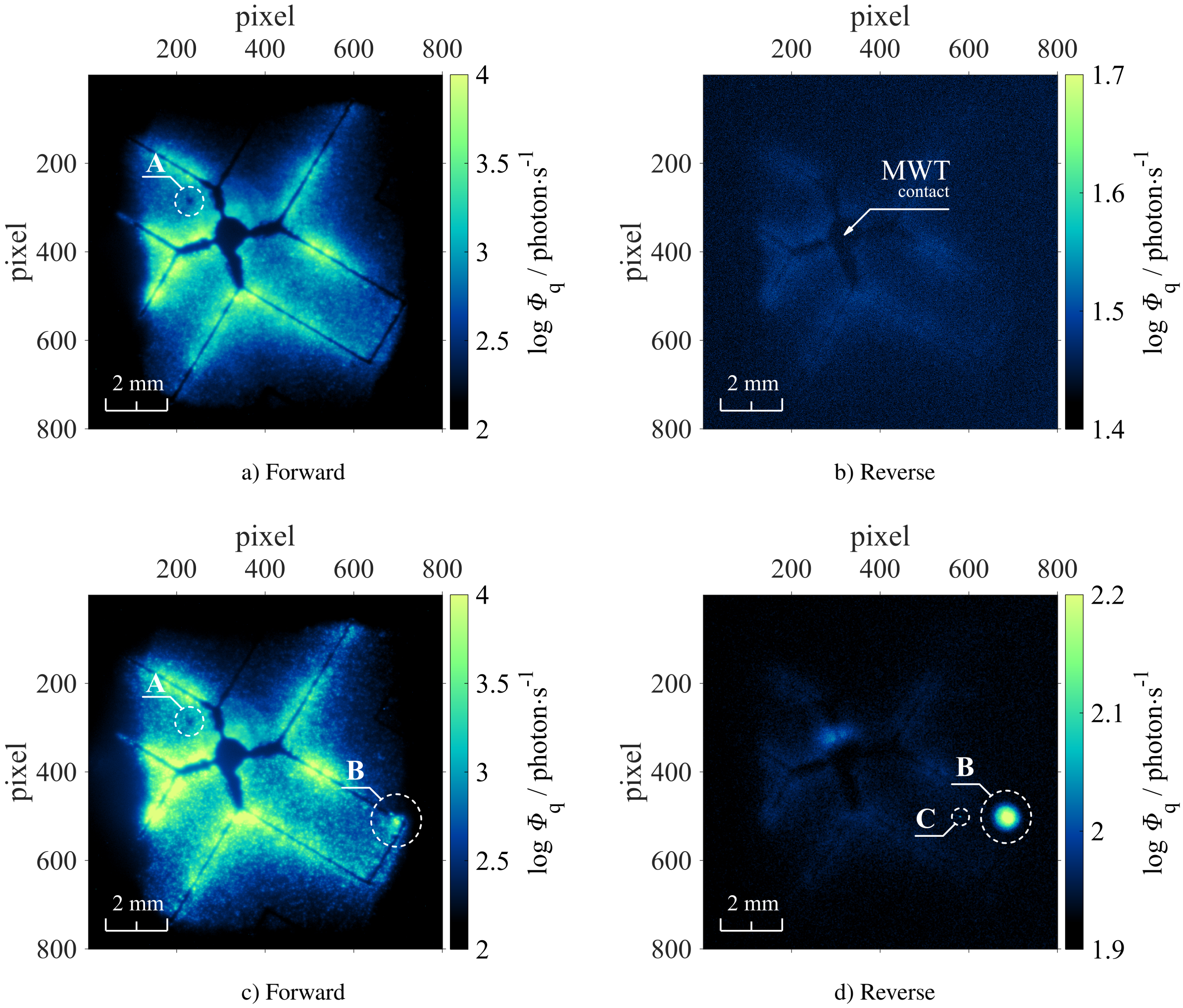

Figure 2: Comparison of electroluminescence intensity maps before and after local breakdown, sample $^{NS}CIGS_3$, area 108.1 mm^2, perimeter 39.6 mm, $T_A = 301.15$ K. a) $U_F = 0.59$ V, $I_F = 10$ mA, b) $U_R = 1.01$ V, $I_R = 10$ mA, c) $U_F = 0.97$ V, $I_F = 35$ mA, d) $U_R = 2.53$ V, $I_R = 35$ mA.

the reverse-bias measurements. As can be seen in Fig. 2b before a creation of local breakdown at a higher voltage there were not any visible defects. Fig. 2d show an electroluminescence map for reverse-bias after a creation of the defect. This defect was marked as “B” and it was also visible under a forward-bias. The influence of this defects was also clearly visible in Fig. 1a of *J–V* characteristics such an increase of reverse current. The defect also had an influence at the forward *J–V* characteristic which is more visible in semilogarithmic scale in Fig. 1b. The minor defect marked as “C” was visible only under reverse-bias. The metalized regions in Fig. 2 were completely dark since no emitted light can go through the metal layer [4]. Electroluminescence sensing by CCD was a powerful tool to actually seen a radiation map of recombination centers. The examination of defects was based on knowledge of shunts types in ordinary c-Si solar cells. The defects were differed by the behavior of their *J–V* characteristics and by their physical origin [5]. Lock-in thermography with electroluminescence allowed a precise analysis whether obtained defects have a linear or a non-linear *J–V* characteristics. The linearity or resistive-like behavior of the microstructure defects characteristics is investigated by comparing electroluminescence intensity or lock-in thermograms at the same bias in forward and reverse condition. The *J–V* characteristics were linear if the shunts show the same thermal or electroluminescence intensity under both conditions. Otherwise, the *J–V*

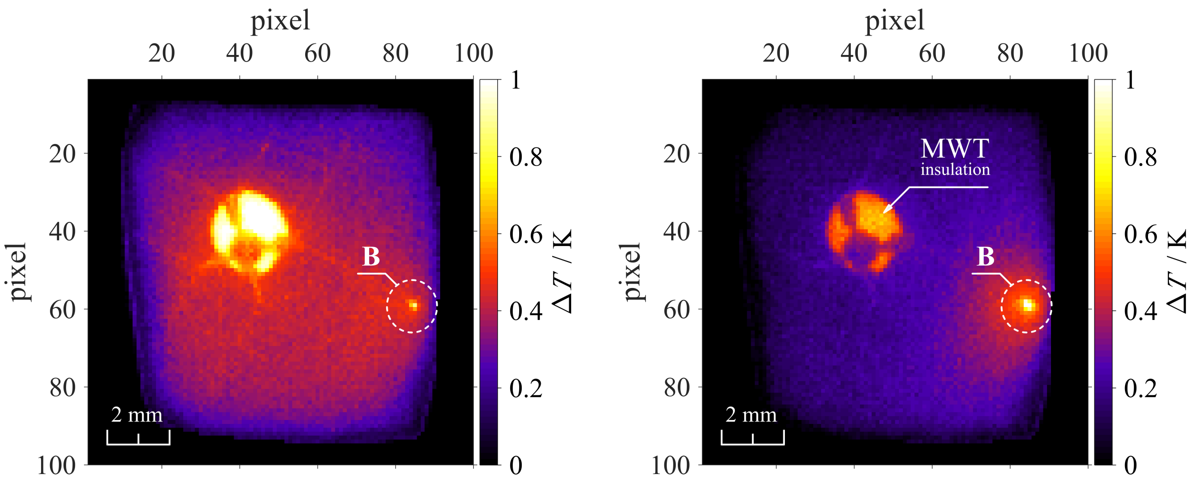

a) Forward b) Reverse

Figure 3: Lock-in thermal images after occurred local breakdown, sample $^{NS}CIGS_3$, T_A = 301.15 K. a) U_F = 1.57 V, I_F = 100 mA, b) U_R = 2.71 V, I_R = 40 mA.

characteristics were a non-linear with a diode-like behavior. The defects in ordinary c-Si solar cells related to a Schottky-type shunts, ohmic shunts, weak-diodes, avalanche and Zener breakdown regions, linear and non-linear edge shunts, cracks and dislocation or areas of high resistance [6, 7]. Areas with a constant EL emission in Fig. 2a were brighter which indicates a good quality deposited layers. Then a dark defect marked as “A” in Fig. 2a corresponded with a poor radiation which indicated defective regions related to crystal inhomogeneities (often visible under reverse-bias for samples $^{NS}CIGS_1$ and $^{NS}CIGS_2$). The obtained defect marked as “B” in Fig. 2a and mainly visible under reverse-bias in Fig. 2c showed a presence also under an IR-lock investigation in Fig. 3 [8]. Fig. 4 showed a cross-section of MWT architecture, multilayer structure and obtained defects on the surface. A sub-layer of $MoSe_2$ is visible in Fig. 4b. The discovered defects in Fig. 4c were a disruption in i-Zno/ZnO:Al layer and exposed CIGS layer due to a undeposited CdS/*i*-Zno/ZnO:Al layer.

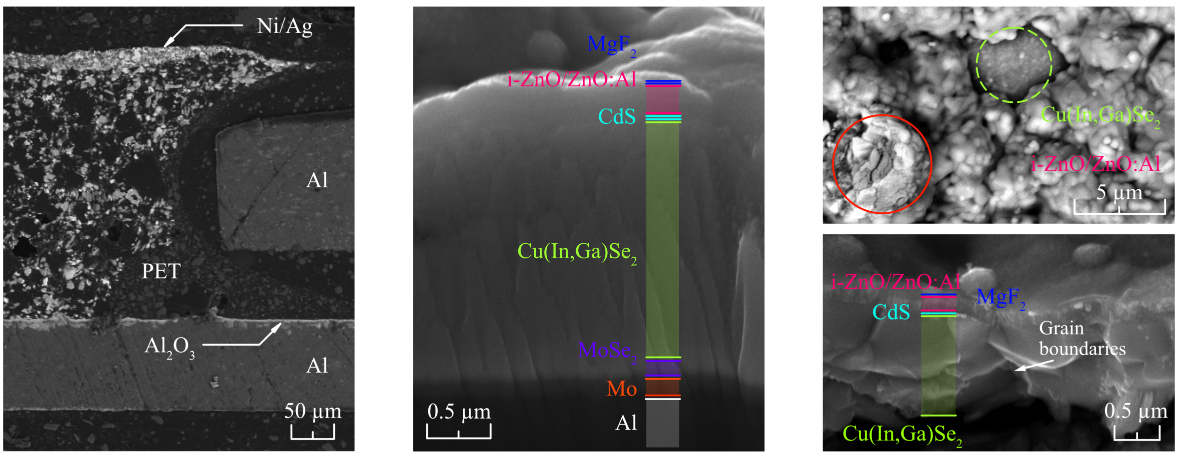

a) b) c)

Figure 4: Chalcophyrite $Cu(In,Ga)Se_2$ solar cell examination under SEM in a micro-scale. a) Cross-section of MWT architecture, BSE, b) FIB cross-section of layers structure, SE, c) surface defects (top image), SE , fractured multilayer structure (bottom image), BSE.

4. CONCLUSION

The electroluminescence as a sensitive method provide a detail intensity map of radiation. The sensed intensity maps showed a different type of radiation under forward and reverse bias. The radiation in forward bias was evenly distributed for a whole sample but more significant intensity was observed in close to the contact grid. Randomly distributed dark spots on the surface were detected despite the evenly distributed radiation at the forward-bias. In contrast, the radiation in reverse bias was detected only from randomly distributed local defects. The some defects obtained by electroluminescence strongly correlates with the defects obtained by lock-in thermography. This electroluminescence and thermal radiation of the presented sample showed a strong dependence at the one particular defect visible mainly under reverse-bias. The real cross-section of multilayer structure and metal wrap through architecture was examined by using the scanning electron microscope in combination with the focused ion beam. A formed sub-layer $MoSe_2$ was identified between the $Mo/Cu(In,Ga)Se_2$ interface. Future work will be focused on detail surface exploration in a micro-scale by scanning electron microscope with a view to determine localized defects by electroluminescence.

ACKNOWLEDGEMENT

This work was supported by the Internal Grant Agency of Brno University of Technology, grant No. FEKT-S-17-4626.

REFERENCES

[1] JACKREL, D., B. CARDOZO, F. JACOB, G. BROWN, P. STONE, J. WOODRUFF, G. KIMBALL, P. JEFFRIES, W. ZHANG, V. FAIFER, and J. KRAWCZYK. Roll-to-roll printer solar cells: Up-scaling from laboratory to megawatts of production. *27th European Photovoltaic Solar Energy Conference and Exhibtion.* 2012, 2249–2253.

[2] PAGLIARO, M., G. PALMISANO and R. CIRIMINNA. *Flexible solar cells.* 2008, pp. 2O2, Weinheim: Wiley-VCH. ISBN 978-3-527-32375-3.

[3] BREITENSTEIN, O., J. P. RAKOTONIAINA and M. H. Al RIFAI. Quantitative evaluation of shunts in solar cells by lock-in thermography. *Progress in Photovoltaics: Research and Applications.* 2003, **11**(8), 515–526.

[4] LÓPEZ, A. B. C., A. M. VEGA a A. L. LÓPEZ. *Next generation of photovoltaics new concepts: new concepts.* 2012, pp. 356, Berlin: Springer. ISBN 978-364-2233-692.

[5] TRAN, T. M. H., B. E. PIETERS, M. SIEGLOCH, A. GERBER, C. ULBRICH, T. KIRCHARTZ, R. SCHÄFFLER and U. RAU. Characterization of Shunts in Cu(In,Ga)Se2 Solar Modules via Combined Electroluminescence and Dark Lock-in Thermography Analysis. *26th European Photovoltaic Solar Energy Conference and Exhibtion.* 2011, 2981–2985.

[6] BREITENSTEIN, O., J. P. RAKOTONIAINA, M. H. AL RIFAI and M. WERNER. Shunt types in crystalline silicon solar cells. *Progress in Photovoltaics: Research and Applications.* 2004, **12**(7), 529–538.

[7] CAO, Q., O. GUNAWAN, M. COPEL, K. B. REUTER, S. J. CHEY, V. R. DELINE and D. B. MITZI. Defects in Cu(In,Ga)Se2 Chalcopyrite Semiconductors: A Comparative Study of Material Properties, Defect States, and Photovoltaic Performance. *Advanced Energy Materials.* 2011, **1**(5), 845–853.

[8] KENDIG, D., G. B. ALERS and A. SHAKOURI. Thermoreflectance imaging of defects in thin-film solar cells. *2010 IEEE International Reliability Physics Symposium.* 2010, IEEE, 499–502.